

## Very Large Scale 3D DC Resistivity Mapping: Inferring the Location of Deep Structural Feeders Beneath Surface Hot-Spring Manifestations

Shore, G.A. <sup>[1]</sup>

1. Crone Geophysics & Exploration Ltd.

### ABSTRACT

*Very Large Scale (VLS) 3D resistivity imaging can be loosely defined as the routine acquisition and 3D inversion investigation of true 3D DC resistivity field data that extend to 3 to 10 times the nominal depth of investigation that is required for imaging some initially conceived target feature. Being basically an extension of 3D imaging to reveal the larger scale context, it also applies laterally. In both dimensions, there is the opportunity not only to better understand the nature and perhaps the genesis of the targeted body, but to discover additional resources of a completely different geophysical signature, scale, orientation or geometry. Successful application of the approach depends upon acquiring a deep field data set that is dense and uniformly distributed both laterally and to depth, and unfaillingly omnidirectional. While some true 3D survey techniques gather field data sets in a (pole-dipole) derivative measurement mode, the imagery shown here derives from the point-potential (pole-pole) measurement mode employed by the 3D E-SCAN DC resistivity system for its greater density of overlapping sampling, its superior depth of investigation and its higher signal return, enabling the acquisition of useful data to effective depths in excess of 5,000 m. This uniform omnidirectional DC resistivity data set supports continuous high resolution 3D inversion results throughout the deeper areas, without having to switch to sparse MT measurements part way down. In this presentation, I show how the deep, highly resolved 3D imagery can assist in inferring the probable location of otherwise geophysically undetectable deep fluid conduits or structures beneath an area hosting multiple hot spring manifestations at surface. The process makes use of exceptionally subtle 3D resolution to image the shallower, detectable imprint of historic hydrothermal fluid flow and related alteration. Mid-depth imagery may identify underlying fluid flow interconnections between separate hot spring manifestations. The imagery supports inferential (logical) identification of the likely location of the deep hydrothermal fluid source that is needed to explain the shallower flow patterns, and appropriate deep drill testing can be planned accordingly. The primary case example involves the Gwenivere and Clementine high-grade gold structures (the Hollister Mine), north Carlin Trend, Nevada.*

### INTRODUCTION

Toward the north end of Nevada's Carlin Trend, the Hollister property has seen decades of exploration effort leading to the present status of well over a million ounces of gold in a basement-hosted feeder vein system. The presence of disseminated gold and alteration in the area's volcanic cover has been known for a long time; the USX open pit remains as visual evidence of the earlier focus on lower-grade, shallow resources. Arrowhead-quality silica sinters are exposed at surface in several areas, and these attracted attention in early days as (presumed) stand-alone hot spring systems. They were drilled locally, mostly vertically, to try to locate feeder structures for their possibly high-grade gold content. Eventually, angled drilling expanded the testing to deeper possibilities, entering the Ordovician basement, and not being restricted to directly below the surficial hot spring sinter manifestations. High-grade, basement-hosted narrow vein intercepts resulted, not under, but between parallel surface sinter deposits. This deep drilling success could have been predicted, and may yet prove useful in targeting deep drilling elsewhere on the property, using Very Large Scale (VLS) 3D resistivity mapping and knowledge of the strategy now in hand.

In this paper, I will start by showing the importance of acquiring high density, uniformly sampled, omnidirectional data at the

appropriate survey scale, in order to produce high quality resistivity data to resolve complex structure and to have confidence in deep or subtle anomalies. These are the essential acquisition parameters in order to infer the location of deep structural feeders. With this essential background, I discuss three examples of deep structural feeder detection, culminating in the primary example of the Hollister Mine, which is a drilled case study.

### THE E-SCAN SYSTEM

The E-SCAN system is a distributed-array 3D induced polarization (IP) and 3D resistivity acquisition and imaging system, employing hundreds of remote-addressable, pre-installed grounded electrodes. E-SCAN is typically used in the pole-pole configuration, though pole-dipole capability has been available. A few of the important features of the system, especially as it was applied to the projects described in this paper, are: its ability to handle any type of terrain due to its simple and flexible wiring requirements; its ability to easily change scale from closely-spaced stations for near-surface detail work to very widely-spaced stations for deep penetration; and its lack of directional bias obtained by rejecting the line-based approach of data collecting, and instead insisting on true omnidirectional readings throughout the grid, with high-density, uniform sampling of the earth both laterally and to depth. Thus,

E-SCAN meets all the essential acquisition parameters mentioned in the previous paragraph.

### DATA COLLECTION AND ANALYSIS

Very Large Scale 3D resistivity imaging is loosely defined as the routine acquisition and 3D inversion investigation of true 3D DC resistivity field data that extend to 3 to 10 times the nominal depth of investigation that is required for imaging some initially conceived target feature. Being basically an extension of coverage to reveal the larger scale context, it also applies laterally. In both dimensions, there is the opportunity not only to better understand the nature and perhaps the genesis of the targeted body, but to discover additional resources of a completely different geophysical signature, scale or orientation.

Successful application of the approach depends upon acquiring a deep field data set that is dense and uniformly distributed both laterally and to depth, and universally omnidirectional. While some true 3D survey techniques gather field data sets in a (pole-dipole) derivative measurement mode, the imagery shown in this paper derives from the point-potential (pole-pole) measurement mode employed by the 3D E-SCAN DC resistivity system for its greater density of overlapping sampling, its superior depth of investigation and its high signal return, enabling the acquisition of useful data to effective sampling depths in excess of 5,000 metres. This provides uniform omnidirectional DC resistivity data sampling and supports continuous high resolution 3D inversion results throughout the deeper areas, without having to switch to sparse magnetotelluric (MT) measurements part way down.

### The Importance of High Density, Uniformly-Sampled Data

Inadequate field data poses difficulties in interpretation, both for the geoscientist observing a field plot such as in Figure 1a, and correspondingly for his digital assistant, the 3D data inversion program. The “simple” task of drawing a connecting line between adjacent anomalies is, in Figure 1a, open to two possibilities: from the west anomaly, connect to the north-east, or to the south-east. Even if one looks outside and finds, for example, SE regional structural trends for guidance, one must commit to the assumption that the local anomalous feature is aligned with the principal regional structure orientation, and is not within or aligned with a possible cross-breaking (NE) fault. An appropriate line spacing (Figure 1b) picks up the intermediate anomaly that confirms a NE linear, while the absence of an intermediate anomaly confirms that the proposed SE orientation is not viable.

Now if you consider the thousands of such decisions which would have to be made by a software program when used on a large set of sparse data, you begin to appreciate the importance of having adequate data. When the 3D complexity of an area becomes greater, or subtler, or both, a program of true 3D data sampling becomes essential for obtaining objective and detailed 3D imagery. Line-based survey techniques, even those with substantial cross-line or off-line data shots, will usually fail to meet basic standards for lateral and vertical uniformity of data

distribution, upon which the objective and reliable generation of subtly resolved true 3D anomaly patterns absolutely depend.

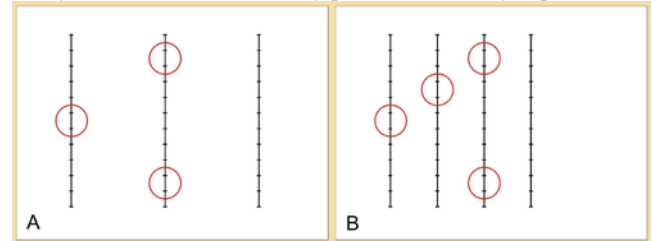


**Figure 1:** Anomalies on lines that are too widely separated (a) and on closer lines (b) that support an objective interpretation by geoscientists, and more importantly, by computers.

### The Importance of Omnidirectional Data

In Figure 2, a principal E-W fault is complicated by cross-breaking faults and a shear zone. The line-based survey at right is deliberately oriented to test the E-W fault, but will miss resolving the almost parallel NNE and NNW faults and shears. A uniformly distributed omnidirectional data set, as at left, provides comprehensive hard-data sampling of the entire complex of structures (and related mineralization) without the need to commit to a specific line orientation to favour one orientation or the other.

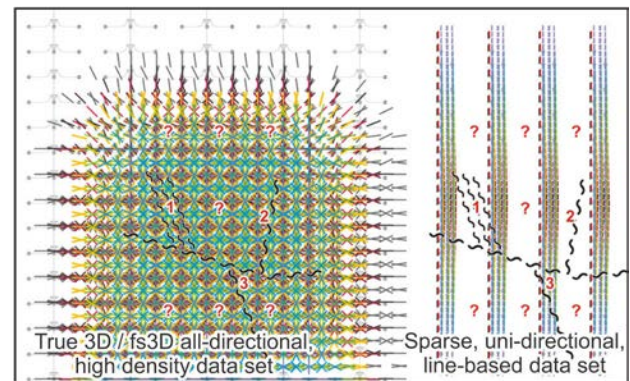


**Figure 2:** True 3D field data sampling vs line-based survey sampling with a depth colour coded tick mark placed at each nominal reading position.

### The Importance of Using a Correct Survey Scale

Figure 3 shows the relative scale of three surveys performed at vastly different scales: with field data effective depth ( $Z_e$ ) changing from 60 m (a), to 600 m (b), and finally to 4100 m (c). Figure 3a shows the close spacing historically employed in the Toodoggone district of north-central British Columbia in the search for metre-wide gold-bearing silicified veins. This 10 m dipole survey would seem to be the correct choice for the target size, but in fact, it proved unsuccessful in detecting mineralization, because there was insufficient contrast with the immediate surrounding host material. Instead, the 100 m grid spacing VLS E-SCAN spacing data set (Figures 3b and 2 left) was successful in locating economic epithermal gold systems in this area by mapping the silicic leakage haloes around the gold-bearing hydrothermal conduits. The haloes had a resistivity two to four times higher than background and were easily detected.

This approach had the effect of increasing the scale of anomaly recognition from a couple of metres (no success) to 100 m to 200 m across in a successful, if small scale, example of VLS 3D resistivity results supporting the inference of a “necessary” feeder structure being present within the larger scale silicified haloes (see Figure 4).

The key was in choosing the correct survey scale to laterally map the resistive halo, from which an inference could be made. With the application of a VLS 3D survey, it was possible to recognize and define the lateral boundaries of the hydrothermal fluid leakage (precipitation-sealed) halo, providing the focus for the detailed drilling required to detect the source conduit structure within. As is recommended to explorationists wherever possible, the VLS strategy was first tested over the nearby producing mine, the Lawyers Deposit, which showed its own 100 m resistive halo and provided confirmation that the VLS strategy was effective for locating that orebody, at least.

Figure 4 shows a 3D-inverted sub-area of Toodoggone survey coverage (VLS resistivity data per Figures 3b and 2 left) in which a 100 m radius silicic leakage halo is seen surrounding the non-economic Duke’s Ridge deposit, a 15 m wide gold-bearing quartz “blow” or pipe. The elongate halo within which the Phoenix Deposit was found suggested coincidence with known area WNW structure trends, which resulted in drilling being oriented NNE at intervals along the long axis. The Phoenix shear is 2 m wide, 60 m long, and featured intervals of >76 oz/ton Au over the 2 m with sweet spots of over 300 oz/ton Au. It was profitably mined. Without this implementation of VLS 3D resistivity strategy being applied here, the high-grade Phoenix deposit would likely have remained undetected.

Finally, Figure 3c shows a VLS 3D resistivity inverted model which has directly and positively imaged the deep fluid vent responsible for supplying the 8 km long active geothermal reservoir above it. Previous knowledge would have skimmed the top of the anomaly, locating the near-surface upward projections and perhaps leading investigators to guess that these projections might be bumps overlying areas of deep upflow. Had these guesses been the only source of guidance, they would have been proven wrong by misplaced deep drilling costing many tens of millions of dollars. With guidance from the unambiguous VLS 3D resistivity mapping, a single 3,000 m borehole can be drilled right down the throat of the accurately located deep vent. Technical details: 400 m by 400 m electrode spacing, additional shallow resolution shots on 400 m x 400 m sub-grid offset 200 m N and 200 m E, maximum delivered current < 2 amperes DC (therefore environmentally benign: no ground disturbance), host resistivity 5–7 ohm-metre; displayed anomaly outer surface 2 ohm-metre, red interior anomaly zones 0.5 ohm-metre. This well-defined 3D conductive anomaly lies in conditions that are hostile for any electrical geophysical survey.

Once again, it was important to choose the appropriate survey scale to achieve these results. The deep (4100 m Ze) data sets density, uniformity of lateral and vertical distribution, and all-directional characteristics remained consistent with the near surface data, with interpretation of strong, deep VLS signals unimpeded by the need for dipole-measuring 3D techniques to

transition to sparse MT data collection in the 1000 m to 1500 m Ze depth of investigation range.

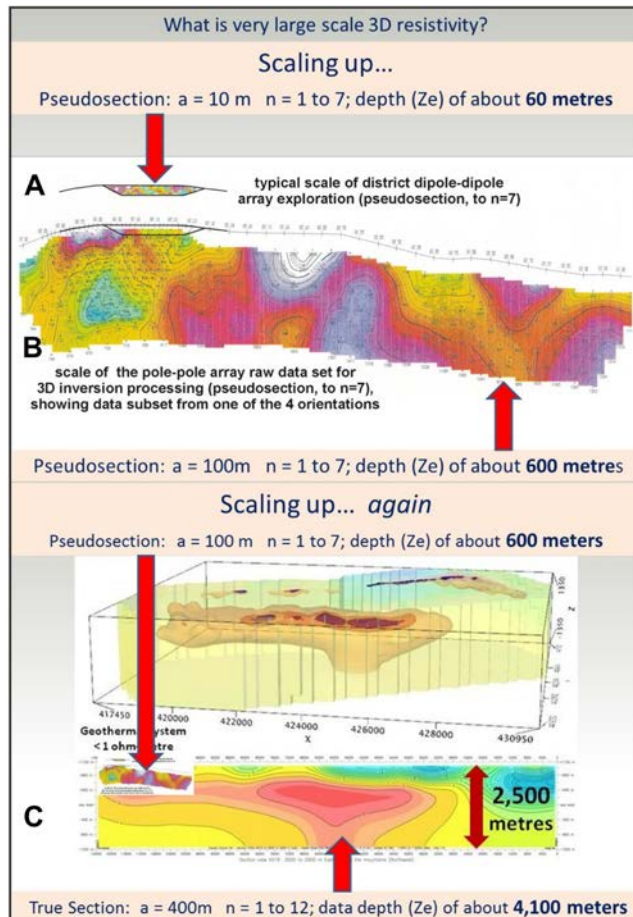


Figure 3: VLS 3D E-SCAN data is acquired by scaling up the electrode grid spacing as needed. No transition to MT data is ever required.

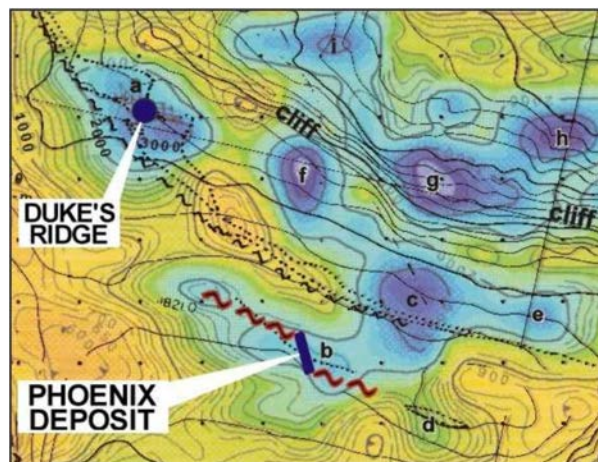
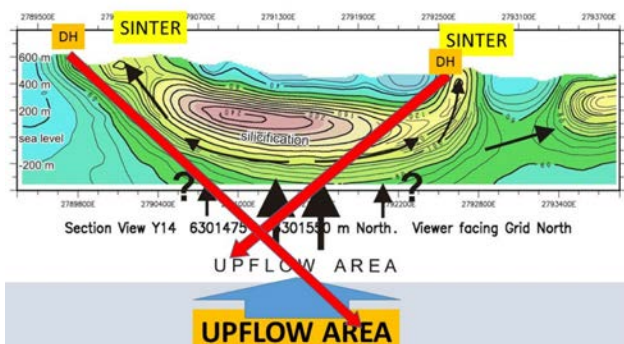


Figure 4: 3D Resistivity inverted model plan view showing high resistivity (blue) anomalies associated with silicic alteration haloes over an 1100 m by 800 m area of Toodoggone volcanics, in central BC.





**Figure 10:** Drilling to test real feeder location, rather than the potential drilling configuration displayed in Figure 8.

The subtlety of VLS 3D resistivity resolution is evident in Figure 11 where the dashed arrows indicate a modest increase in resistivity associated with the two smaller erosional remnants (minor leakage) located between the two big ones. In a system this large, even the minor leakage vent areas may be individually prospective.

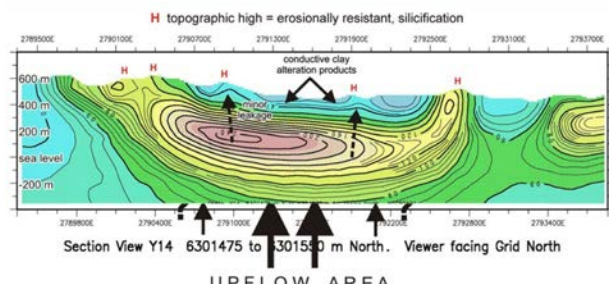


**Figure 11:** The subtle image of minor leakage to smaller sinters.

**Subtle Anomaly Detection**

Back in Nevada, Figure 12 shows a smaller unexplained and untested pattern, located 2600 m southeast of the Hasbrouck Peak deposit, south of Tonopah (Shore and Lymburner, 2015).

At a 4x anomaly ratio against background, in an area where known ore-grade mineralization is at least 20x background, this feature remained unrecognized for 20 years in graphics that focused on just the high ratio anomaly features. After recent reprocessing, this now-recognized feature is estimated at over 1000 m wide by over 400 m tall. A significant amount of fluid has passed through this system, enough to support substantial gold deposition. Neither an anomaly’s ratio to background nor it’s absolute value are independently indicative of the type or potential grade of mineralization represented by this (or any) anomaly, leaving this “weak” VLS 3D resistivity anomaly in unquestionable demand of follow-up. This is an example of how true 3D resistivity data, meeting all the requirements discussed in the **Introduction**, can produce the quality of inversion required to recognize and confirm such subtle anomalies.

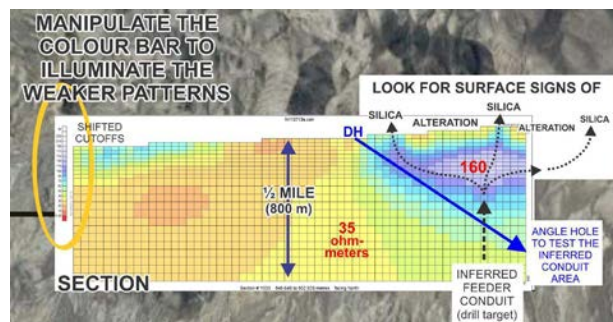


**Figure 12:** Unexplained hydrothermal pattern near Hasbrouck Peak NV.

**The Hollister Mine Example**

While the previous examples may be compelling in theory, it is useful to anchor such thinking with an actual drilled case study. A fully drilled example follows. It is not a VLS 3D resistivity discovery, though the 3D geophysics was completed well in advance of the developments that led to recognition of a significant potential gold producer in the basement rocks. Historic exploration and drilling information are combined with the 3D resistivity results.

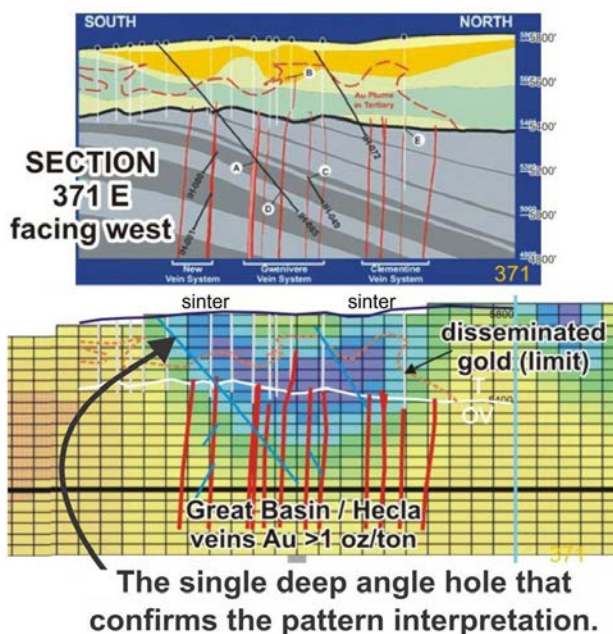
The geophysical and geological images shown here date from the 1990s and do not represent the current state of the resource, but do serve to adequately illustrate the VLS 3D resistivity exploration premise. While it is too late to benefit the known Hollister Mine deposit, the proven VLS resistivity imaging strategy is timely for consideration elsewhere on this property, and more generally, wherever volcanic-hosted epithermal systems are being explored. Note that 3D IP data, collected at the same time on this property, responded to sulphides associated with some of the shallower disseminated gold zones, but provided no assistance in the recognition of the need for the presence of the deep feeder structures.

Figure 13 is a section across the Hollister Mine (Ivanhoe Mining District), now owned by Klondex Mines Ltd. and located in Elko County, approximately 130 km (~80 mi.) northeast of the town of Winnemucca, Nevada and 29 km (~18 mi.) southeast of the Midas Mine. The Hollister Mine is a very well preserved low-sulfidation, epithermal gold-silver deposit associated with mid-Miocene bimodal volcanism of the Northern Nevada Rift.

Figure 13 shows 300 ft to 400 ft (~91 m to ~122 m) of volcanics covering the Ordovician Valmy basement, which hosts the principal silicic gold-bearing veins known as Gwenivere and Clementine. The resistive (blue) U-shaped anomaly extends upward from the interface between the basement rocks and the overlying Tertiary volcanics. The two resistive “arms” that sweep upward to surface are interpreted as the fossil traces marking the pathways of substantial historic thermal fluid upflow, with some precipitation of a sealant (silica, but carbonate would present the same imagery) along the way. The existence of prominent sinter deposits in the areas where the “arms” reach surface supports this interpretation.

The broad base of the U-shaped resistive anomaly, sitting on the interface between the volcanics and tight basement siltstones,

invites explanation as a self-sealing silica cap precipitated by thermal fluids rising in basement faults. As the fluids are delivered into the more permeable volcanics, they experience depressurization and boiling. As the precipitated silica seals off the volcanics locally, the continuously rising thermal fluids are forced laterally within the volcanics, extending the width of the precipitated seal until the fluids have sufficiently cooled and/or depleted their solution load, whereupon they can rise toward the surface where they vent as hot springs, creating the sinter deposits. The elevated resistivity marking the full U-shaped pattern represents the fossil trace of these fluid pathways. Each part may potentially host gold values. In addition to the prospect for bonanza grade gold deep in the vertical feeders, one must acknowledge the potential for Hishikari style mineralization along the boiling zone at the lower edge of the precipitated cap, and for disseminated gold deposition through each of the several distinctive pattern components of the 3D imagery, including the plume traces, the bulk of the cap itself, and the (probably) altered volcanics lying between the cap and surface.



**Figure 13:** Geophysically undetectable feeders in the basement.

In accepting such a hydrologic model as explaining the observed pattern, we establish a need for the existence of the basement feeder structures of some type, independent of whether we can “see” them with geophysics or not. Usually, we cannot see such veins or conduits because they are volumetrically too small, so we can only hope to infer their most likely location.

In a simplest case, there would be one conduit fault or intersection (effective pipe) centered below the deepest-extending part of the resistive anomaly pattern. The reality of several parallel fault zones underlying this Hollister anomaly serves to warn us that more complex source structures, and perhaps multiple fluid pulse sequences, may be present beneath any similar anomaly expression, so that in every exploration case going forward, the possibility of multiple source conduits (and pulses) must be allowed. In any case, those conduit

sources most directly associated with creation of the “U” anomaly should be located beneath the width of the anomaly, i.e. the precipitated cap.

In Figure 14, the Hollister Mine principal veins (in red) are flanked at surface by subtle, parallel, elevated resistivity anomalies representing the trace of hydrothermal fluids venting at surface along most of the length of the deep vein system. Other parallel linear resistivity anomalies are visible throughout the property, representing possible duplications of the conditions seen over the Gwenivere and Clementine vein systems. These are near-surface, fine details, which I suggest would not be obtained except through the gathering of a high density, uniformly distributed and omni-directional field data set. In this case the 3D survey electrode grid spacing was 400 ft by 400 ft (~122 m by ~122 m); data being of the pole-pole array variety. Most of the 3D field data (3D IP and 3D resistivity) behind these images was gathered during the 1990s.

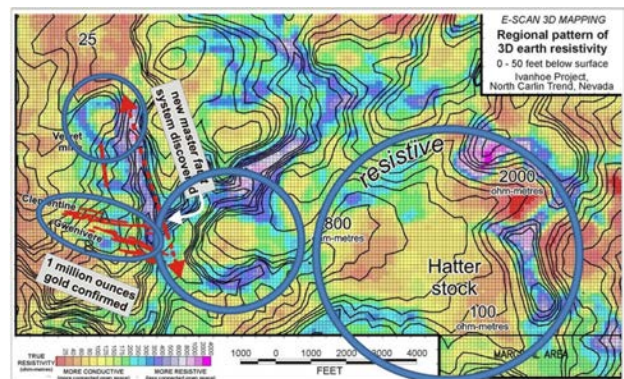


**Figure 14:** From the 3D resistivity inverted model, this plan view at surface shows the Gwenivere and Clementine vein systems, containing >1 million ounces of gold, shown in red at left.

The elongate nature of the U-shaped anomaly, as it tracks the entire length of the Hollister Mine veins, is more clearly seen in Figure 15 (below) where four adjacent N-S sections are observed crossing the predominantly E-W gold vein structures. Since 2000, there has been some drilling in the areas marked as “not drilled at depth”.

The linear resistive traces at surface, and the circular traces at “F” and possibly “E” of Figure 16, mark the surface venting areas for rising thermal waters whose ascending pathways are interpreted to have been laterally diverted by the self-sealing effects of a locally precipitated silica cap, whether elongate or circular.

Drilling beneath the E-W linear features is accomplished by stepping back and drilling N or S as in the Hollister Mine example. The circular resistive feature at Butte-Velvet “F”, complete with nearby historic mercury workings, probably represents a pipe-like or fault-intersection conduit, which requires a more comprehensive drilling strategy to ensure intersection of the vertical conduit that must underlie this pattern somewhere at depth.

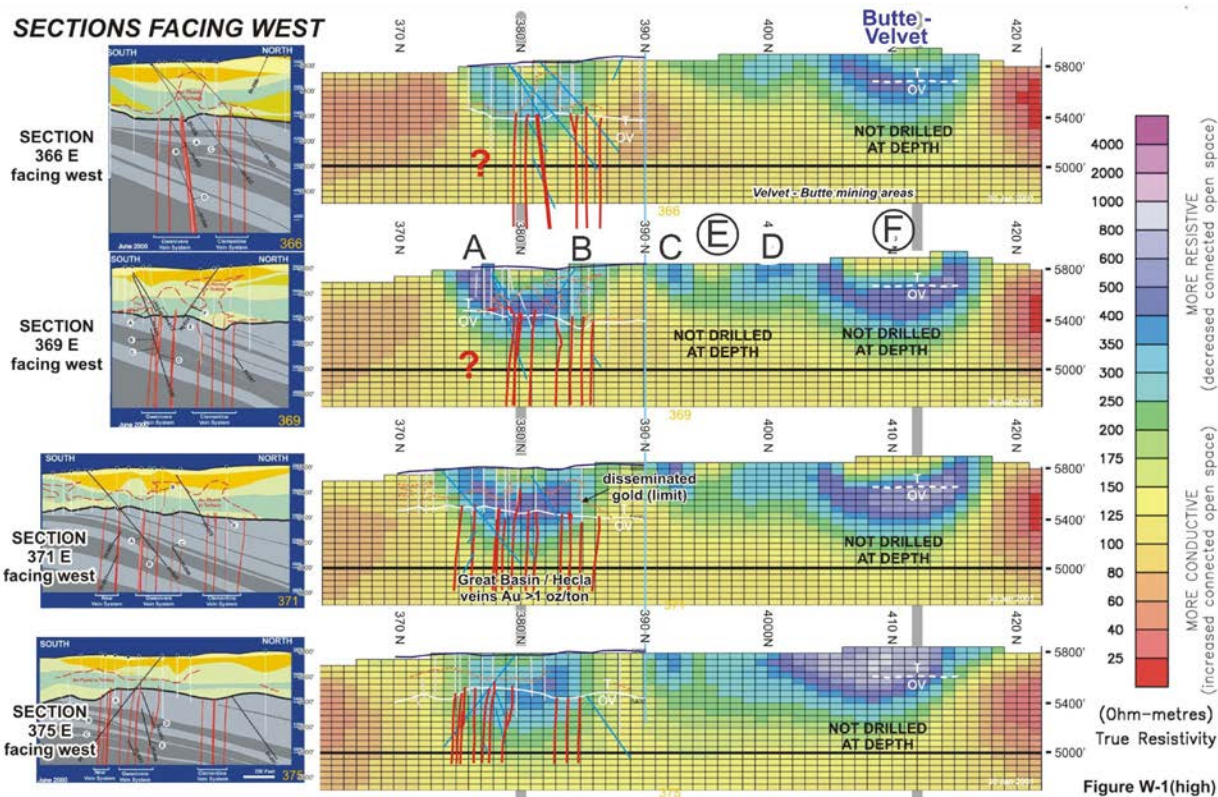


**Figure 15:** The sequence of sections illustrates the linear continuity of the pattern of deep silica precipitation and the lateral (N-S) diversion of upward fluid flow along the Gwenivere-Clementine fault system (at left). Circular patterns located at Butte-Velvet to the north had not been drilled at the time of creation of this circa-2000 3D imagery.

**RECENT DEVELOPMENTS**

The VLS 3D resistivity strategy has been applied in an Archean setting, where fossil traces of hydrothermal fluid movement were observed rising to surface, in quite different rocks, and from a different deep fluid source mechanism image. We are cautiously optimistic that this experience may be expanded not just across other Archean settings, but potentially as a long-awaited deep-pattern-based method of discrimination within the busy and confusing electrical geophysical patterns that are typical of sedimentary hosted gold settings, e.g. Nevada’s Carlin Trend.

**CONCLUSION**

In some cases, VLS 3D resistivity mapping can effectively locate for drilling those geophysically invisible deeper conduits and feeders which overlying 3D imagery indicates must exist in order to complete a plausible epithermal/hydrologic model.

**REFERENCE**

Shore, G.A. and J. Lyburner, 2015, 3D Resistivity characterization of the Hasbrouck Peak epithermal gold system: a district shallow-exploration signature, <http://www.cronegeophysics.com/wp/wp-content/uploads/2015/06/GSN-Hasbrouck-2panels-36inch-tall-200dpi.pdf>, accessed 31 January 2017.

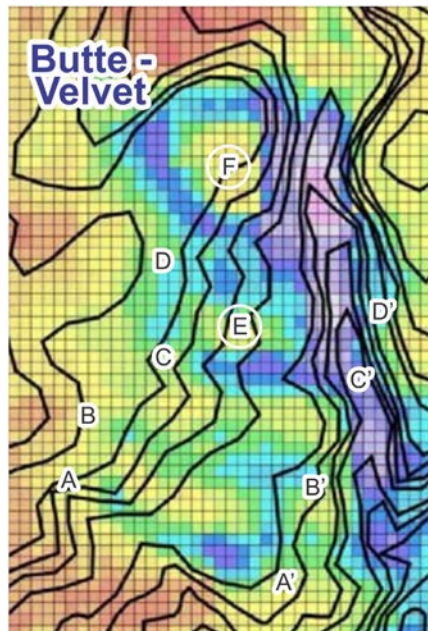


**Figure 16:** Surface traces of U-shaped elevated resistivity for the several parallel U-shaped patterns of Figure 15.